

Analysis of minimum distribution time of two-class tit-for-tat-based P2P file distribution

Masahiro Sasabe*, Masaki Kiyomitsu

*Nara Institute of Science and Technology,
8916-5 Takayama-cho, Ikoma, Nara 630-0192, Japan*

Abstract

The demand for large-scale file distribution over the Internet has been increasing, such as software and its update data distribution. When a new and/or popular file is released, many users tend to simultaneously access distribution server(s), making them bottleneck. Several systems (e.g., Windows Update) have started applying the peer-to-peer (P2P) file distribution paradigm where users' devices (i.e., peers) assist the file distribution. Since peers will consume their access link capacities to upload fragments of the file (i.e., pieces) to others, an appropriate incentive mechanism should be designed to motivate peers to behave cooperatively. In this paper, we focus on the tit-for-tat (TFT) based P2P file distribution with two-class peers where equivalent amount of piece exchange between each pair of peers is guaranteed and peers are classified into two classes: peers with high upload capacity or those with low one. In particular, given the system parameters (e.g., the number of peers and the upload capacity distribution), we specify the bottleneck of the system and derive the corresponding minimum file distribution time, with the help of fluid model. Through numerical results, we verify the validity of analytical results and compare the system performance of TFT based P2P file distribution with that of existing architectures: client-server file distribution and cooperative P2P file distribution.

Keywords: Peer-to-peer file distribution, tit-for-tat strategy, minimum distribution time, fluid model

1. Introduction

The demand for large-scale file distribution over the Internet has been increasing, such as software and its update data distribution (e.g., Ubuntu Linux [1] and Windows Update [2]). When a new and/or popular file is released, many users tend to simultaneously access distribution server(s), which causes flash crowds [3] and makes them bottleneck. To reduce the load on servers, several systems, e.g., Ubuntu Linux, Windows Update, and Amazon Simple Storage Service (Amazon S3), have started applying the peer-to-peer (P2P) file distribution paradigm where users' devices (i.e., peers) assist the file distribution.

In the P2P file distribution, a file is divided into fragments (i.e., pieces) and peers can download pieces from not only the server but also other peers. However, it has been pointed out that many peers are prone to be free riders who retrieve pieces from others but do not provide any piece to others [4]. One of the possible reasons causing the free-riding behavior is the upload capacity consumption by providing pieces to others, which may degrade the quality of other network services that the corresponding user enjoys. To alleviate the free-riding problem, several P2P

file distribution systems, e.g., BitTorrent [5], apply the tit-for-tat (TFT) strategy in game theory [6]. In P2P file distribution systems, the TFT strategy can be regarded as equivalent amount of pieces exchanged between each pair of peers.

Recently, the optimality of the TFT-based P2P file distribution and the optimal piece flow have been analyzed [7, 8, 9, 10]. The piece flow describes the transfer timing of each piece from a node (i.e., server or peer) to a peer. In [7], the authors first modeled the TFT-based P2P file distribution as a discrete-time system and formulated the optimal piece-flow determination problem to minimize the average file distribution (download) time as an integer linear program (ILP). They also obtained the optimal solutions using the existing solver, i.e., CPLEX [11], and investigated the distribution mechanisms of the server and peers to yield the optimal piece flow. This ILP-based approach can precisely analyze the piece-level system behavior but has the potential drawback of computational complexity, which makes difficult to analyze large-scale systems directly.

In case of the cooperative P2P file distribution, which relies on the altruistic peers' behavior and does not consider the TFT strategy, Kumar et al. derived explicit expressions for the minimum file distribution time with the help of fluid model [12]. Inspired by [12], the author formulated the optimization problem for minimizing the file

*Corresponding author

Email addresses: m-sasabe@ieee.org (Masahiro Sasabe),
kiyomitsu.masaki.kd2@is.naist.jp (Masaki Kiyomitsu)

distribution time of the TFT-based P2P file distribution¹⁰⁵ as a linear program (LP) [10]. The author also obtained the optimal solutions using CPLEX and analyzed the system performance of the TFT-based P2P file distribution.
 55 This LP-based approach overcome the scalability issue in the ILP-based approach and succeeded in directly analyz-¹¹⁰ ing large-scale systems, e.g., a few thousands nodes, under arbitrary upload capacity distribution. However, it cannot give us the explicit formula that presents the relationship
 60 between the system parameters (e.g., the number of peers and the upload capacity distribution) and the minimum¹¹⁵ file distribution time of the TFT-based P2P file distribution. We expect that deriving the explicit formula is important to predict appropriate equipment investment (e.g., server's upload capacity) by considering the balance be-
 65 tween the system performance (i.e., file distribution time)¹²⁰ and investment cost.

In this paper, inspired by [10, 12], we newly develop a fluid model to analyze the minimum file distribution time
 70 of the two-class TFT-based P2P file distribution where only two-class peers (i.e., peers with high upload capacity¹²⁵ and those with low one) exist. In particular, given the system parameters, we specify the bottleneck of the system and derive the corresponding minimum file distribution
 75 time. Through numerical results, we verify the validity of analytical results and compare the system performance of¹³⁰ TFT-based P2P file distribution with that of existing architectures: client-server file distribution and cooperative P2P file distribution without TFT constraint.

The rest of the paper is organized as follows. Section 2
 80 gives related work. In Section 3, we describe the system¹³⁵ model of the two-class TFT-based P2P file distribution and derive its minimum file distribution time in Section 4. After describing numerical results in Section 5, we give
 85 conclusions in Section 6.

2. Related work

Since P2P file distribution relies on the assistance of peers, the system behavior of P2P file distribution tends to be more complex than that of client-server file distri-
 90 bution, due to selfish/rational behavior of individual peers (free riding [4] and peer churn [13]) and/or introduction of incentive mechanisms [14] (e.g., economy-based mech-
 95 anisms [15], exchange-based reciprocity mechanisms like TFT strategy [16], and reputation-based mechanisms [17,¹⁵⁰ 18]). Therefore, revealing the performance (e.g., distribution time and throughput) of P2P file distribution has attracted more attention continuously [19, 20].

In this paper, we also tackle this problem by newly developing a fluid model to analyze the minimum distri-
 100 bution time of two-class TFT-based P2P file distribution under the flash crowds where steep access concentration on the server occurs. (The detail will be given in Section 4.) In this section, we introduce related work similar to our approach from various aspects.
 160

At first, from the viewpoint of system model, many studies on performance evaluation of TFT-based P2P file distribution have focused on one of the representative systems, i.e., BitTorrent [12, 21, 22, 23, 24, 25, 26, 27]. In [21], the authors proposed a simple fluid model to derive average file download time under the assumptions that peers with uniform upload capacity arrive at the system following a Poisson process, stay the system during the time following an exponential distribution, and leave the system. In [22], the authors proposed a fluid model that can reproduce the phenomenon that peers with uniform upload capacity have heterogeneous download time, which was observed by simulations under the same assumptions in [21]. In [23], the authors proposed a queuing network model to analyze the impact of system parameters and strategies selecting peers and pieces for retrieval on system throughput under the assumptions that peers with uniform upload capacity arrive at the system following a Poisson process whose arrival rate exceeds the server's upload capacity and leave the system just after file downloading.

In [24], the authors identified that the utilization of the available bandwidth of peers can be classified into three phases over the course of file downloading through the measurement study of BitTorrent on PlanetLab [28, 29] under the assumptions that peers with heterogeneous upload capacities simultaneously participate in the system and leave the system immediately after file downloading. They further proposed an analytical model to study the impact of bandwidth utilization on the system performance under flash crowds. In [25], using this measurement-driven analytical model, the authors investigated four different server distribution policies to reduce the server's upload capacity without increasing the file download time.

In [26], under the assumptions that peers with heterogeneous upload capacities arrive at the system following a Poisson process and leave the system just after file downloading, the authors proposed a fluid model to derive the transition of the number of peers under file downloading. In [12], the authors proposed a fluid model to derive the minimum file distribution time under the assumptions that peers with heterogeneous upload capacities simultaneously finish file downloading. This analysis targets for a single file and its extension for multi-file cases can be found in [27].

These existing studies focused on modeling and performance evaluation of BitTorrent(-like) systems without directly considering the TFT strategy in the analytical approaches. In recent years, several studies tried to reveal the impact of the TFT strategy on the system performance of P2P content (i.e., file or streaming) distribution by modeling the system behavior in piece-level granularity [7, 8, 9, 30, 31]. In [30], the authors analytically derived the minimum file distribution time by modeling the flow of pieces with TFT constraints under the assumptions that peers with uniform upload capacity simultaneously start and finish file downloading. The piece-level analysis of the TFT-based P2P content distribution was also conducted

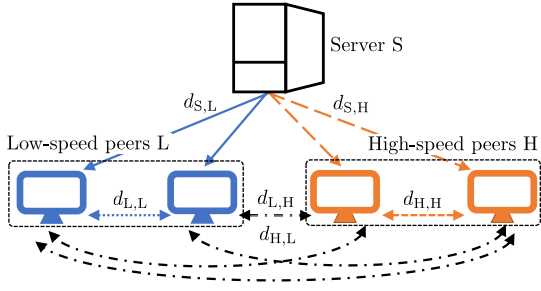


Figure 1: Example of system configuration ($N = 4, \alpha_H = 0.5$).

using ILP-based approaches [7, 8, 9, 31]: minimization of average file download time [7], minimization of average play-out delay in streaming [31], analysis of optimal P2P topology for content distribution [8], and optimality analysis of locality-aware TFT-based P2P file distribution [9].¹⁶⁵ These ILP-based approaches can precisely analyze the system behavior in piece-level granularity and provide us with some important insights about optimal distribution mechanisms of server and peers. They, however, cannot directly deal with large-scale systems, due to computational com-¹⁷⁰plexity.

In [10], inspired by the fluid model in [12], the author formulated an LP to minimize the file distribution time of TFT-based P2P file distribution under the assumptions that peers with heterogeneous upload capacities simultaneously start and finish file downloading. This LP-based approach can deal with larger-scale systems, e.g., a few thousands of peers, thanks to the existing solver. However,¹⁷⁵ the explicit relationship between system parameters (e.g., the number of peers and upload capacity distribution) and minimum file distribution time has not been revealed yet.

In this paper, inspired by the fluid model in [12] and the LP-based approach in [10], we aim at deriving the minimum file distribution time of the two-class TFT-based P2P file distribution.¹⁸⁰

3. System model

We consider a two-class TFT-based P2P file distribution system that consists of one *server* S with upload capacity U_S ($U_S > 0$) and N ($N \geq 1$) *peers* denoted by $\mathcal{N} = \{1, \dots, N\}$. Note that the one virtual server can also be regarded as a set of multiple servers. Peers are divided into two classes: $\alpha_H N$ ($0 \leq \alpha_H \leq 1$) peers with high upload capacity U_H (i.e., *high-speed peers*), denoted by \mathcal{N}_H , and $(1 - \alpha_H)N$ peers with low upload capacity U_L (i.e., *low-speed peers*), denoted by \mathcal{N}_L ($U_H > U_L > 0$). Note that nodes are homogeneous in each group, and thus we collectively refer to high-speed (resp. low-speed) peers as H (resp. L) for simplicity of description. Hereafter, the server and peers are referred to as *nodes*. Fig. 1 illustrates an example of system configuration with $N = 4$ and $\alpha_H = 0.5$.¹⁹⁰ In what follows, for simplicity of analysis in Section 4, we assume that high-speed peers and low-speed ones are more

than one, respectively (i.e., $2 \leq \alpha_H N \leq N - 2, N \geq 4$).²⁰⁵ Considering the fact that the uplink capacity tends to be much smaller than the download one in the current Internet connections, we assume that the bottleneck will occur at the upload capacity of certain node(s) in the system.

We consider the following flash crowds situation. At the initial state ($t = 0$), the server S holds a file of size F ($F > 0$) while all the peers do not have any portion of the file. Note that peers are called *leechers* if they do not complete the file download. Leechers will complete file downloading by retrieving different portion of the file from the server as well as other peers, and finally become *seeds*, which are peers with the entire file. As for the distribution mechanism, we follow the same assumption in the fluid-model based analysis of minimum distribution time of P2P file distribution [12]. To be more precise, the server divides the file into N variable-size blocks where N is the same as the number of peers, and distributes them through N application-level multicast trees where i th tree is rooted in the server S , passes through the leecher i , and terminates at each of the remaining $N - 1$ leechers, as shown in Fig. 1. Thanks to the fluid model, we assume that each leecher i can replicate and forward a bit as soon as it receives the bit. Different from the assumption in the existing work [12], we force each pair of leechers to exchange equal amount of bits to ensure the TFT strategy.²¹⁰

In this paper, as in [12], we consider a situation where all the peers simultaneously retrieve file at a constant bit rate d ($d > 0$), which can be regarded as one possible situation that can easily be controlled by the server. Note that the download (resp. upload) rate from high-speed peer $i \in \mathcal{N}_H$ to low-speed peer $j \in \mathcal{N}_L$ may be different even under the identical download rate d among all the peers. (We will show the details in Section 4.) Since the peers in each group (i.e., high-speed and low-speed) are homogeneous, the download rate of high-speed (resp. low-speed) peer becomes identical and is denoted by d_H (resp. d_L).²¹⁵ d_H, d_L , and d should satisfy

$$d_H = d_L = d. \quad (1)$$

The download rate d_H of a high-speed peer is the sum of that from the server, that from other high-speed peers, and that from low-speed peers. We can also obtain the download rate d_L of a low-speed peer in a similar manner. As result, d_H and d_L are given as follows:

$$d_H = d_{S,H} + (\alpha_H N - 1)d_{H,H} + (1 - \alpha_H)N d_{L,H}, \quad (2)$$

$$d_L = d_{S,L} + ((1 - \alpha_H)N - 1)d_{L,L} + \alpha_H N d_{H,L}, \quad (3)$$

where $d_{i,j}$ ($i \in \{S, H, L\}, j \in \{H, L\}$) is the download rate from node i to peer j .

To achieve the fastest file distribution, the server's upload capacity should be fully utilized. On the other hand, the upload rate of high-speed peer and that of low-speed peer should be equal or less than the corresponding upload capacity. These can be expressed by the following

Table 1: Notations.

Notation	Definition
N	Number of peers, $\mathcal{N} = \{1, \dots, N\}$
α_H	Fraction of high-speed peers ($0 \leq \alpha_H \leq 1$)
U_S	Upload capacity of server S
U_H	Upload capacity of high-speed peer
U_L	Upload capacity of low-speed peer ($U_H > U_L > 0$)
d_H	Download rate of high-speed peer
d_L	Download rate of low-speed peer
d	Download rate of peer ($d_H = d_L = d$)
$d_{i,j}$	Download rate from node $i \in \{S, H, L\}$ to leecher $j \in \{H, L\}$
F	File size
T	Distribution time ($T = F/d$)

constraints:

$$\alpha_H N d_{S,H} + (1 - \alpha_H) N d_{S,L} = U_S, \quad (4)$$

$$(\alpha_H N - 1) d_{H,H} + (1 - \alpha_H) N d_{H,L} \leq U_H, \quad (5)$$

$$((1 - \alpha_H) N - 1) d_{L,L} + \alpha_H N d_{L,H} \leq U_L. \quad (6)$$

In addition, each download rate should be nonnegative:

$$d_{i,j} \geq 0, \quad i \in \{S, H, L\}, j \in \{H, L\}. \quad (7)$$

Focusing on the bit-level data retrieval, we have to ensure that each leecher can provide other leechers with bits retrieved from the server:

$$d_{H,H} \leq d_{S,H}, \quad (8)$$

$$d_{L,L} \leq d_{S,L}, \quad (9)$$

$$d_{H,L} \leq d_{S,H}, \quad (10)$$

$$d_{L,H} \leq d_{S,L}. \quad (11)$$

In addition, we require the following TFT constraint:

$$d_{H,L} = d_{L,H}. \quad (12)$$

Finally, Table 1 summarizes the notations used in this paper.

4. Minimum distribution time analysis of two-class TFT-based P2P file distribution

In this section, focusing on the bottleneck in the system, we will derive the relation between the system parameters (i.e., the number N of peers, the fraction α_H of high-speed peers, and upload capacities of nodes, U_S , U_H , and U_L) and minimum file distribution time. The bottleneck cases can be divided into the following three cases. If the upload capacity of server is insufficient, all peers cannot fully utilize their upload capacities (case C1). If we gradually increase the upload capacity of server, the next case C2 will appear, where low-speed peers can fully utilize their upload capacities but high-speed peers cannot. Further increase of the upload capacity of server will lead to the last case C3 where all peers can fully utilize their upload capacities. In what follows, we will derive explicit expressions for the conditions and minimum distribution time of each case using the system parameters.

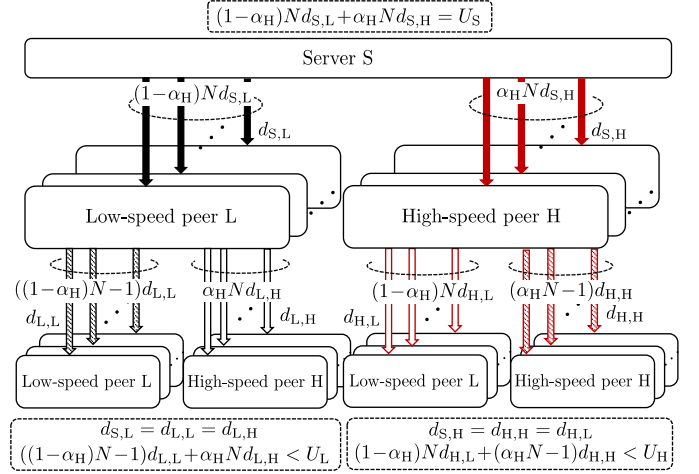


Figure 2: C1: Server's upload capacity is bottleneck for all peers.

4.1. C1: Server's upload capacity is bottleneck for all peers

Fig. 2 depicts the flow relationship between nodes in case C1. Since the upload capacity of server becomes the bottleneck for all peers in case C1, from the viewpoint of the uniqueness of retrieved content, $d_{H,H} = d_{S,H}$ and $d_{L,L} = d_{S,L}$ hold for the download rate between high-speed peers and that between low-speed peers, respectively. Similarly, the download rate between high-speed peer and low-speed peer should satisfy

$$d_{H,L} = d_{L,H} = \min(d_{S,H}, d_{S,L}). \quad (13)$$

Assuming $d_{S,H} \leq d_{S,L}$, from (1), (2), and (3), we obtain

$$d_{S,H} = d_{S,L} = d_{L,L} = d_{H,H} = \frac{U_S}{N}. \quad (14)$$

Under the opposite assumption, i.e., $d_{S,H} \geq d_{S,L}$, we also obtain (14). As a result, from (1), (2), and (14), the download rate becomes $d = U_S$, and thus the minimum distribution time T_{TFT} of two-class TFT-based P2P file distribution (i.e., *TFT model*) is given by

$$T_{\text{TFT}} = \frac{F}{d} = \frac{F}{U_S},$$

which is the same as the minimum distribution time T_{ALT} of cooperative P2P file distribution (i.e., *cooperative model*) [12].

Finally, we derive the conditions of C1 using the system parameters. Since the strict inequality should hold in (5) and (6), respectively, (13) and (14) give us

$$U_S < \frac{N}{N-1} U_H, \quad (15)$$

$$U_S < \frac{N}{N-1} U_L. \quad (16)$$

Next, we focus on (7)–(12). Since the right side of (13) and that of (14) become positive, respectively, (7) is satisfied for all the pair of nodes, and thus (8)–(11) always hold.

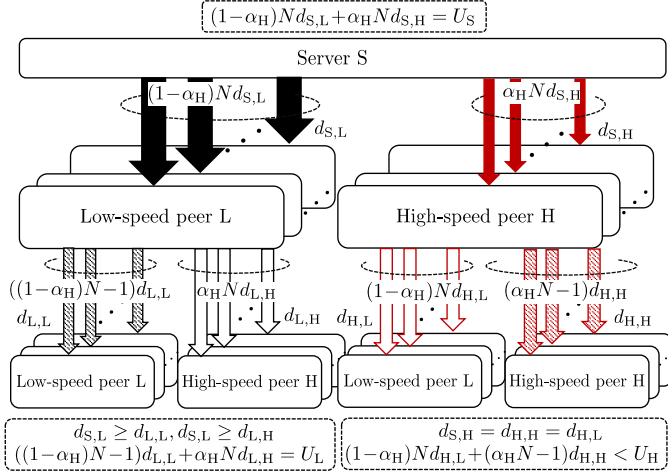


Figure 3: C2: Server's upload capacity is bottleneck only for high-speed peers.

So far we have obtained all the individual conditions and found that (15) and (16) are the final conditions. Since the right side of (15) is greater than that of (16) because of $U_H > U_L$, the condition of C1 is given by (16).

4.2. C2: Server's upload capacity is bottleneck only for high-speed peers

Next, Fig. 3 presents the flow relationship between nodes in case C2. In this case, the minimum download time T_{ALT} of cooperative model is given as follows [12]:

$$T_{ALT} = \frac{F}{\min(N^{-1}U_S + \bar{U}_P, U_S)}, \quad (17)$$

where \bar{U}_P is the average upload capacity among peers, i.e., $\alpha_H U_H + (1 - \alpha_H)U_L$.

In case of TFT model, the upload capacity of server becomes the bottleneck for the high-speed peers, which gives

$$d_{H,H} = d_{S,H}. \quad (17)$$

In addition, the low-speed (resp. high-speed) peers can (resp. cannot) fully utilize their upload capacities, and thus (6) (resp. (5)) satisfies equality (resp. strict inequality) condition.

From (3) and (6), the download rate d_L of low-speed peer is determined by $d_{L,L}$ and $d_{L,H}$. On the other hand, from (5) and (12), we observe that the increase of $d_{L,H}$ will more contribute to the download rate of high-speed peer than that of $d_{L,L}$, and thus the following conditions should hold:

$$\begin{aligned} d_{L,H} &= \min(d_{S,H}, d_{S,L}) \quad \text{if } d_{L,L} > 0, \\ d_{L,H} &\leq \min(d_{S,H}, d_{S,L}) \quad \text{if } d_{L,L} = 0. \end{aligned} \quad (18)$$

In what follows, we continue the analysis by dividing C2 into two sub-cases: C2-a where $d_{L,L} > 0$ and C2-b where $d_{L,L} = 0$. Note that the derivation of conditions for C2 will be given in Appendix B.

4.2.1. C2-a: $d_{L,L} > 0$

In this case, from (18), $d_{L,H} = \min(d_{S,H}, d_{S,L})$ holds. In addition, $d_{S,H} \leq d_{S,L}$ is derived according to proof by contradiction (See the detail in Appendix A). As a result, we obtain the following condition:

$$d_{H,H} = d_{S,H} = d_{H,L}. \quad (19)$$

Next, focusing on the equality condition in (6), we obtain the following conditions from (1), (2), (4), and (19):

$$d_{S,H} = \frac{U_S + (1 - \alpha_H)NU_L}{(\alpha_H + (1 - \alpha_H)N)N}, \quad (20)$$

$$d_{S,L} = \frac{U_S - \alpha_H U_L}{\alpha_H + (1 - \alpha_H)N}. \quad (21)$$

From the equality condition in (6), $d_{L,L}$ is given as follows:

$$d_{L,L} = \frac{(\alpha_H + (1 - \alpha_H)^2 N)U_L - \alpha_H U_S}{(\alpha_H + (1 - \alpha_H)N)((1 - \alpha_H)N - 1)}. \quad (22)$$

From (1), (3), (19), (20), (21), and (22), we have

$$d = \frac{U_S + (1 - \alpha_H)NU_L}{N - \alpha_H N + \alpha_H},$$

which gives the minimum distribution time T_{TFT} of TFT model:

$$T_{TFT} = \frac{F}{d} = \frac{(N - \alpha_H N + \alpha_H)F}{U_S + (1 - \alpha_H)NU_L}.$$

4.2.2. C2-b: $d_{L,L} = 0$

Because of $d_{L,L} = 0$ and the equality condition in (6), we have

$$d_{L,H} = \frac{U_L}{\alpha_H N}. \quad (23)$$

As for $d_{S,H}$ and $d_{S,L}$, from (1), (2), (3), (4), (17), and the equality condition in (6), we have

$$d_{S,H} = \frac{\alpha_H U_S + (2\alpha_H - 1)(1 - \alpha_H)NU_L}{\alpha_H^2 N(N - \alpha_H N + 1)}, \quad (24)$$

$$d_{S,L} = \frac{\alpha_H U_S - (2\alpha_H - 1)U_L}{\alpha_H(N - \alpha_H N + 1)}. \quad (25)$$

From (1), (2), (17), and (24), the download rate d becomes

$$d = \frac{\alpha_H U_S + (1 - \alpha_H)(\alpha_H N + 1)U_L}{\alpha_H(N - \alpha_H N + 1)},$$

which gives the minimum download time T_{TFT} of TFT model as follows:

$$T_{TFT} = \frac{F}{d} = \frac{\alpha_H(N - \alpha_H N + 1)F}{\alpha_H U_S + (1 - \alpha_H)(\alpha_H N + 1)U_L}.$$

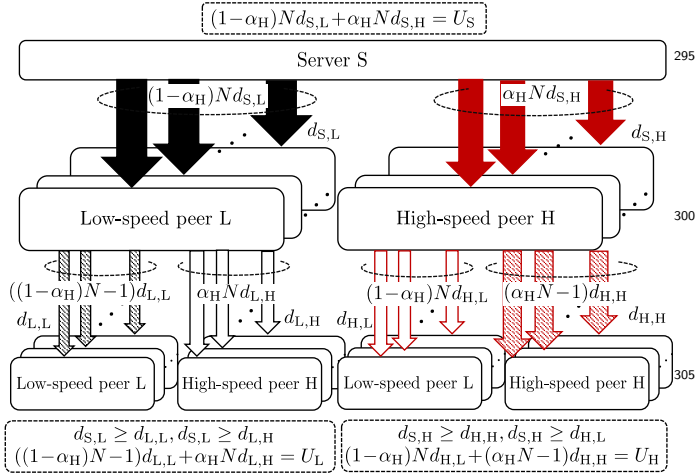


Figure 4: C3: Server's upload capacity is sufficient for all peers.

4.3. C3: Server's upload capacity is sufficient for all peers

Finally, Fig. 4 illustrates the flow relationship between nodes in case C3. In this case, all peers can fully utilize their upload capacities, and thus the equality conditions are satisfied in (5) and (6), respectively. As a result, from (2), (3), and (4), we obtain

$$d_{S,H} = N^{-1}U_S - (1 - \alpha_H)(U_H - U_L), \quad (26)$$

$$d_{S,L} = N^{-1}U_S + \alpha_H(U_H - U_L). \quad (27)$$

From (1), (2), (26), and the equality condition in (5), we obtain the download rate d as follows:

$$d = N^{-1}U_S + \alpha_H U_H + (1 - \alpha_H)U_L = N^{-1}U_S + \bar{U}_P.$$

As a result, the minimum download time T_{TFT} of TFT model becomes

$$T = \frac{F}{d} = \frac{F}{N^{-1}U_S + \bar{U}_P},$$

which is the same as the minimum download time T_{ALT} of cooperative model [12].

The derivation of conditions for C3 will be given in Appendix C.

4.4. Discussion

The minimum distribution time of TFT model and that of cooperative model for each case (i.e., C1, C2-a, C2-b, and C3) can be summarized in Table 2. For comparison purpose, we also show that of client-server (CS) model. Since only the server S distributes the file of size F to all the N peers in CS model, its minimum distribution time T_{CS} is given by FN/U_S , regardless of cases.

We first observe that two P2P models (i.e., TFT model and cooperative model) can achieve more scalable distribution, in terms of the number N of peers, than CS model, regardless of cases. Focusing on the performance of two P2P models, we confirm that TFT model achieves the same

performance as cooperative model in C1 and C3. On the other hand, in C2-a and C2-b, assuming that α_H , U_S , U_H , and U_L are constant and the number of peers is sufficiently large ($N \rightarrow \infty$), we obtain $\lim_{N \rightarrow \infty} T_{\text{TFT}} = F/U_L$ and $\lim_{N \rightarrow \infty} T_{\text{ALT}} = F/\min(\bar{U}_P, U_S)$. Focusing on the conditions for C2-a and C2-b in Table 2, we confirm $U_L < U_S$. In addition, from the definition of \bar{U}_P , we have $U_L < \bar{U}_P$. As a result, $T_{\text{TFT}} > T_{\text{ALT}}$ holds in C2-a and C2-b. Note that TFT model in case 2 is still scalable in terms of N because $T_{\text{TFT}} = F/U_L$ is independent of N .

Next, we focus on the conditions for each case (i.e., C1, C2-a, C2-b, and C3), which are summarized in Table 3¹. Here, we can derive the conditions for C2 (C2-a and C2-b) and C3 in a manner similar to the way used for C1 in Section 4.1. The detail derivation process of C2 and C3 is given in Appendix B and Appendix C, respectively. Despite of the relatively simple structure of the two-class TFT-based P2P file distribution, the resulting conditions for each case show somewhat complicated. However, we observe that the conditions for each case have an interesting hierarchical structure where the conditions for α_H , U_H/U_L , and U_S are considered in this order.

From the viewpoint of scalability, many readers would be more interested in the large-scale systems. In case of $N \rightarrow \infty$, we have $1 - \frac{\sqrt{N-1}}{N} \rightarrow 1$, $1 - \frac{2}{N} \rightarrow 1$, $\theta_1 \rightarrow \frac{1}{\alpha_H}$, and $\theta_2 \rightarrow 1$, which indicates that the shaded area in Table 3 tends to take place.

5. Numerical results

5.1. Evaluation scenario

We consider a P2P file distribution system where one server S distributes a file of 1 [GB] ($F = 8000$ [Mbits]) to 1000 peers ($N = 1000$). At the initial state ($t = 0$), the server S has the entire file while all the peers do not have any portion of the file. We fix the upload capacity U_L of low-speed peer to be 100 [Mbps] while we change U_H/U_L in the range of (1, 100] and set U_S to be 10^k ($k = 2, \dots, 6$).

5.2. Verification of analytical results

To verify the validity of TFT model, we compare the minimum distribution time T_{TFT} of TFT model with that of LP-based approach (LP model), i.e., T_{LP} [10]. LP model aims to directly solve an LP that has the decision variables $d_{i,j} \geq 0$ ($i \in \{S, H, L\}$ and $j \in \{H, L\}$), the same constraints (1)–(12), and the same objective function of $\min F/d$. Fig. 5 illustrates the transition of T_{TFT} and T_{LP} when changing U_S , U_H/U_L , and α_H . We can see from Fig. 5 that T_{TFT} matches to T_{LP} under the same parameter settings.

In addition, given system parameters, TFT model first calculates the corresponding bottleneck case and then derives the minimum distribution time for that case. On the

¹ $N \geq 5$ is required for $\frac{2}{N} < \frac{\sqrt{N-1}}{N}$.

Table 2: Minimum distribution time for each case ($\bar{U}_P = \alpha_H U_H + (1 - \alpha_H) U_L$).

	C1	C2-a	C2-b	C3
TFT model	$\frac{F}{U_S}$	$\frac{(N - \alpha_H N + \alpha_H) F}{U_S + (1 - \alpha_H) N U_L}$	$\frac{\alpha_H (N - \alpha_H N + 1) F}{\alpha_H U_S + (1 - \alpha_H) (\alpha_H N + 1) U_L}$	$\frac{F}{N^{-1} U_S + \bar{U}_P}$
Cooperative model	$\frac{F}{U_S}$	$\frac{F}{\min(N^{-1} U_S + \bar{U}_P, U_S)}$		$\frac{F}{N^{-1} U_S + \bar{U}_P}$
CS model	$\frac{F N}{U_S}$			

Table 3: Conditions for each case ($\theta_1 = \frac{N-1}{\alpha_H N}, \theta_2 = \frac{(1-\alpha_H)(\alpha_H N-1)}{\alpha_H(N-\alpha_H N-1)}, N \geq 5$).

		$\frac{2}{N} \leq \alpha_H \leq 1 - \frac{\sqrt{N-1}}{N}$			$1 - \frac{\sqrt{N-1}}{N} < \alpha_H \leq 1 - \frac{2}{N}$
C1	$\theta_1 < \frac{U_H}{U_L}$	$U_S < \frac{N}{N-1} U_L$	$\theta_2 < \frac{U_H}{U_L}$	$\theta_2 < \frac{U_H}{U_L}$	Same as in $\frac{2}{N} \leq \alpha_H \leq 1 - \frac{\sqrt{N-1}}{N}, \theta_1 < \frac{U_H}{U_L}$
C2-a		$\frac{N}{N-1} U_L \leq U_S < \frac{1}{\alpha_H} (\alpha_H + (1 - \alpha_H)^2 N) U_L$			
C2-b		$\frac{1}{\alpha_H} (\alpha_H + (1 - \alpha_H)^2 N) U_L \leq U_S < \frac{\alpha_H N (N - \alpha_H N + 1)}{\alpha_H N - 1} U_H - \frac{(1 - \alpha_H) N (\alpha_H^2 N - \alpha_H + 1)}{\alpha_H (\alpha_H N - 1)} U_L$			
C3		$\frac{\alpha_H N (N - \alpha_H N + 1)}{\alpha_H N - 1} U_H - \frac{(1 - \alpha_H) N (\alpha_H^2 N - \alpha_H + 1)}{\alpha_H (\alpha_H N - 1)} U_L \leq U_S$			
		$\frac{2}{N} \leq \alpha_H \leq 1 - \frac{\sqrt{N-1}}{N}$			$1 - \frac{\sqrt{N-1}}{N} < \alpha_H \leq 1 - \frac{2}{N}$
C1	$\theta_1 < \theta_2$	$U_S < \frac{N}{N-1} U_L$	$\theta_2 < \frac{U_H}{U_L}$	$\theta_1 < \frac{U_H}{U_L}$	$U_S < \frac{N}{N-1} U_L$
C2-a		$\frac{N}{N-1} U_L \leq U_S < \frac{(N - \alpha_H N + \alpha_H) N}{N-1} U_H - (1 - \alpha_H) N U_L$			
C2-b		—			
C3		$\frac{(N - \alpha_H N + \alpha_H) N}{N-1} U_H - (1 - \alpha_H) N U_L \leq U_S$			
		$\frac{1}{2} < \alpha_H \leq 1 - \frac{\sqrt{N-1}}{N}$			$1 - \frac{\sqrt{N-1}}{N} < \alpha_H \leq 1 - \frac{2}{N}$
C1	$\theta_2 < \theta_1$	$U_S < \frac{N}{N-1} U_L$	$\theta_1 < \frac{U_H}{U_L}$	$\theta_1 < \frac{U_H}{U_L}$	Same as in $\frac{1}{2} < \alpha_H \leq 1 - \frac{\sqrt{N-1}}{N}, 1 < \frac{U_H}{U_L} < \theta_2$
C2-a		$\frac{N}{N-1} U_L \leq U_S < \frac{(N - \alpha_H N + \alpha_H) N}{N-1} U_H - (1 - \alpha_H) N U_L$			
C2-b		—			
C3		$\frac{(N - \alpha_H N + \alpha_H) N}{N-1} U_H - (1 - \alpha_H) N U_L \leq U_S$			

other hand, LP model does not consider the bottleneck cases and directly solves the LP under the given system parameters. This indicates that the classification of cases in TFT model is also correct.

5.3. Relation between system parameters and bottleneck cases

Fig. 6 illustrates the relationship between system parameters and case classification of TFT model, which can be calculated by Table 3. At first, focusing on the impact of U_S , we observe that C1 dominates in case of $U_S = U_L$ (Fig. 6a). Then, we find from Figs. 7b through 7e that the case gradually transitions from C2-a, C2-b, and C3, with increase of U_S . In particular, C2-a and C2-b tend to take place in the wide range of U_S . C3 only occurs when U_S is large, i.e., $U_S \geq 100000$, and lower U_H/U_L and/or higher α_H contribute to its occurrence.

5.4. Impact of TFT strategy on system performance

Fig. 7 illustrates how the system parameters affect the minimum distribution time of TFT model and that of cooperative model. In case of $U_S = U_L$ (Fig. 7a), the bottleneck case becomes C1 as shown in Fig. 6a. In this case,

the server's upload capacity U_S becomes bottleneck and TFT model achieves the same performance as cooperative model as shown in Table 2. If U_S increases, we observe from Figs. 7b through 7d that TFT model (resp. cooperative model) gradually (resp. speedily) reduces the minimum distribution time. Finally, they show the same performance again when $U_S = 1000000$ (Fig. 7e).

Fig. 8 presents the performance ratio of TFT model to cooperative model, i.e., T_{TFT}/T_{ALT} . Since T_{ALT} can be regarded as the lower bound of T_{TFT} , T_{TFT}/T_{ALT} can take the value in the range of $[1, \infty)$ and smaller value means that TFT model is more competitive with cooperative model. In this evaluation scenario, we observe from Figs. 8a through 8e that T_{TFT}/T_{ALT} ranges from 1 to 54 and takes the maximum in case of $U_S = 10000$, $\alpha_H = 0.77$, and $U_H/U_L = 100$. Note that even in such cases TFT model is still much scalable than CS model, which requires minimum distribution time proportion to the number N of peers (See Table 2).

6. Conclusions

In this paper, we have developed a fluid model to analyze the minimum distribution time of the two-class tit-

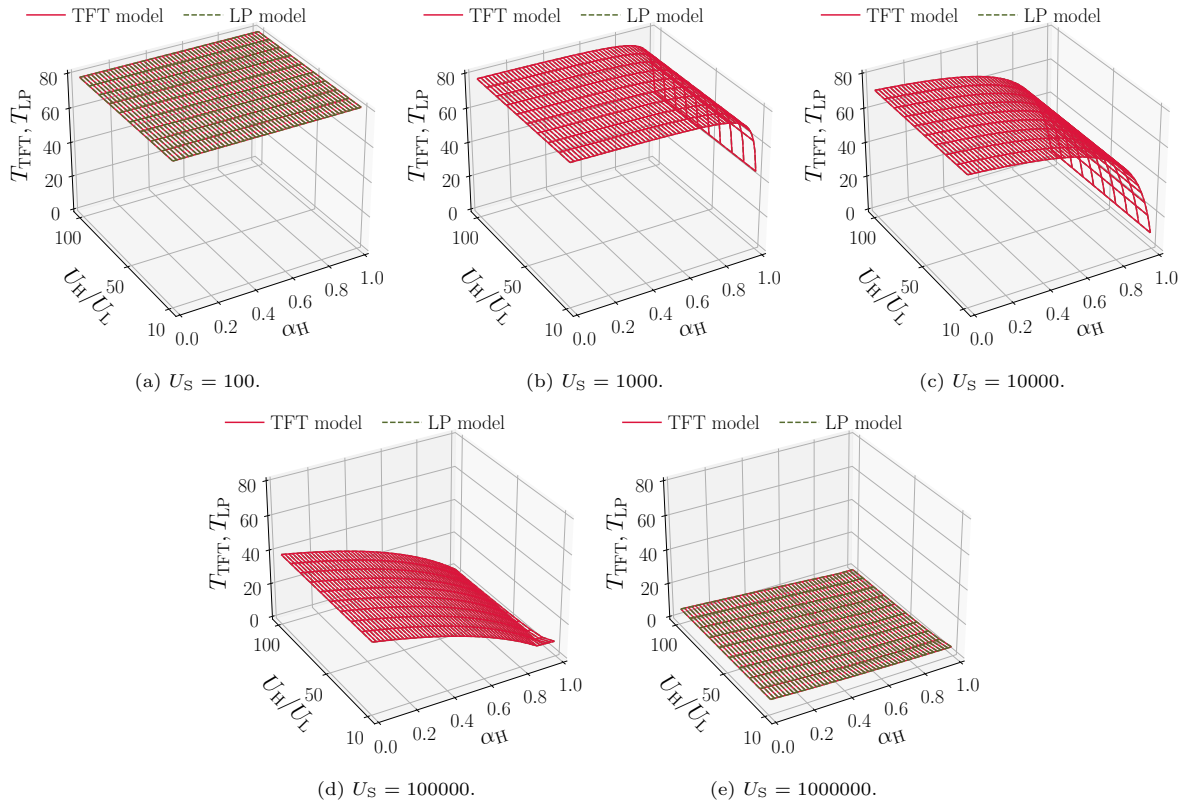


Figure 5: Minimum distribution time of TFT model and LP model.

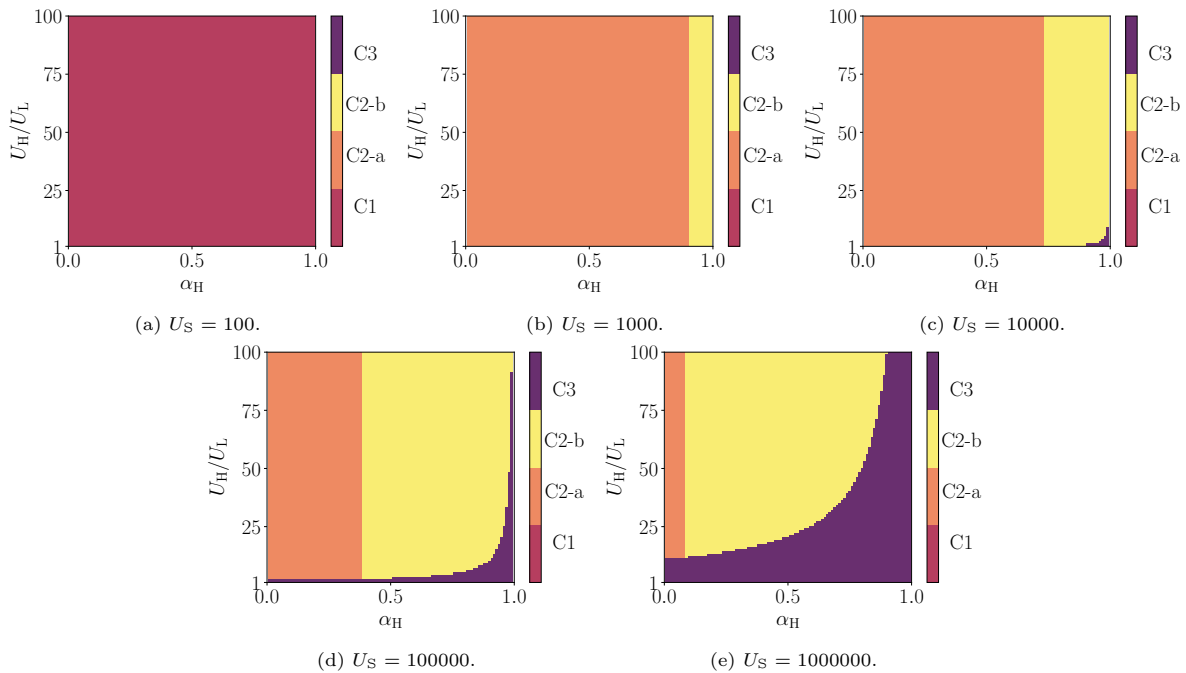


Figure 6: Relationship between system parameters and case classification.

for-tat (TFT) based P2P file distribution where only two-class peers (i.e., high-speed peers and low-speed peers) exist. In particular, given the system parameters (e.g., the number of peers and the upload capacity distribution), we

have revealed that the system bottleneck can be categorized into four cases, which are defined by the conditions for the fraction α_H of high-speed peers, the ratio U_H/U_L of upload capacity between high-speed peer and low-speed

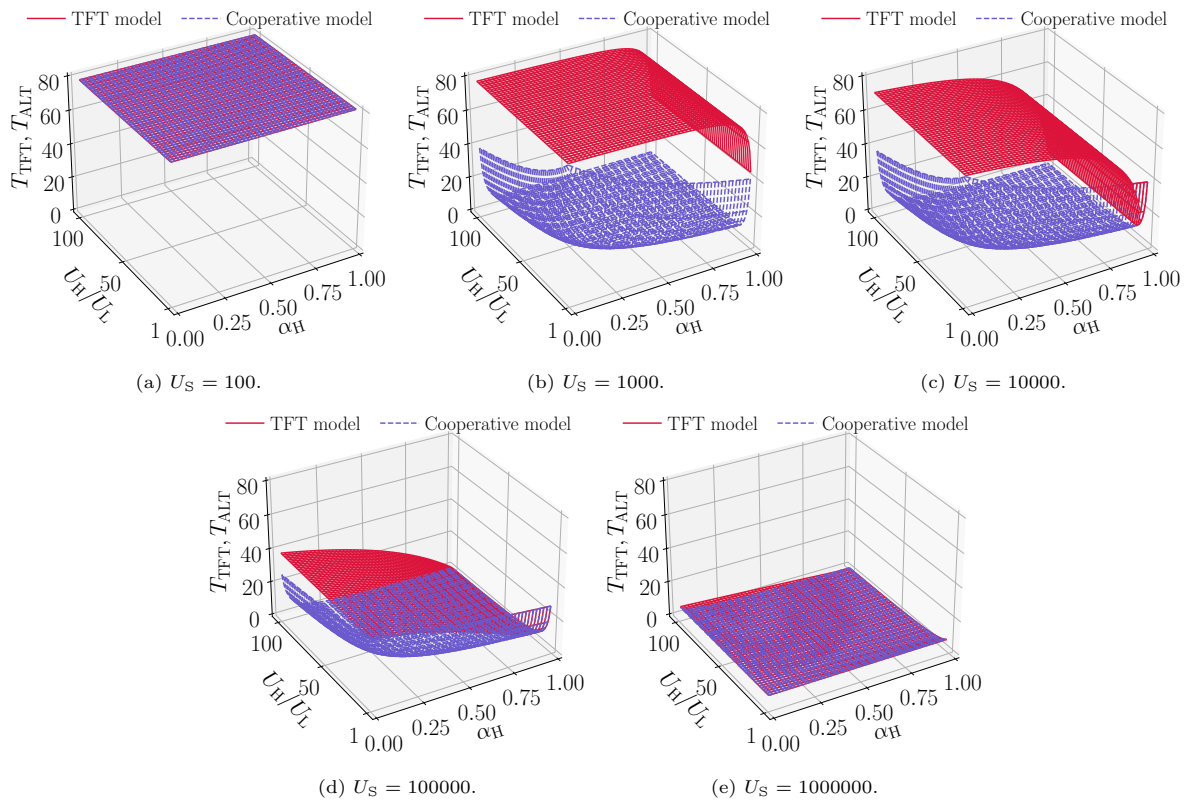


Figure 7: Relationship between system parameters and minimum distribution time (TFT model and cooperative model).

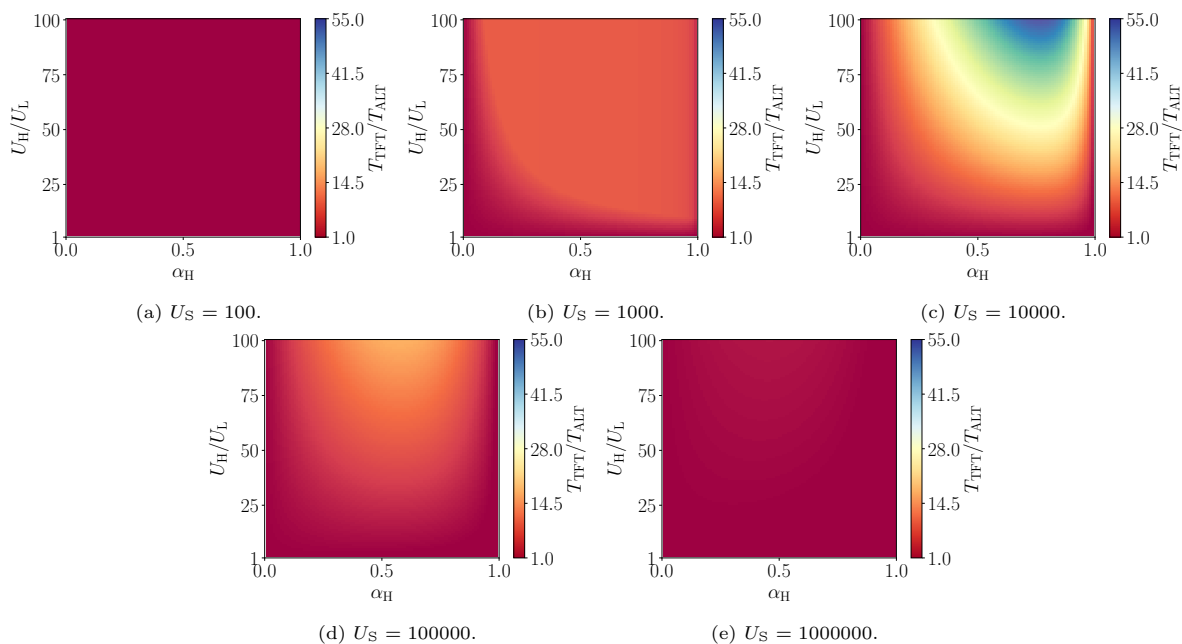


Figure 8: Performance ratio of TFT model to cooperative model.

395 peer, and the server's upload capacity U_S . We have fur-400
 401 ther derived the minimum distribution time for each case.
 402 As a result, we have found that TFT model achieves the
 403 same performance as cooperative model when the server's
 404 upload capacity becomes or does not become bottleneck

for all peers. In other cases, TFT model has larger min-
 405 imum distribution time than cooperative model but it is
 406 still much scalable than client-server (CS) model.

Through numerical results, we have verified the valid-
 407 ity of TFT model by comparing with the existing linear

programming (LP) model under the same assumptions and parameter settings. We have also shown several numerical examples to demonstrate the fundamental characteristics of TFT model through comparison with cooperative model and CS model. In future work, we plan to extend the analytical model to support more general upload capacity distribution.

Appendix A. Proof of $d_{S,H} \leq d_{S,L}$ in C2-a

Lemma 1. In C2-a, $d_{S,H} \leq d_{S,L}$ is satisfied.

Proof. We use proof by contradiction. Assume that $d_{S,H} > d_{S,L}$. From (18), we have

$$d_{H,L} = d_{S,L}. \quad (\text{A.1})$$

From (2), (17), and (A.1), the download rate of high-speed peer becomes

$$d_H = \alpha_H N d_{S,H} + (1 - \alpha_H) N d_{S,L} \quad (\text{A.2})$$

On the other hand, the low-speed peer fully utilizes its upload capacity U_L in C2-a, and thus

$$d_L = d_{S,L} + U_L \quad (\text{A.3})$$

is satisfied.

From (1), (A.1), (A.2), and (A.3), we have

$$d_{S,H} = \frac{(1 - \alpha_H) N U_L - ((1 - \alpha_H) N - 1) U_S}{\alpha_H N}, \quad (\text{A.4})$$

$$d_{S,L} = U_S - U_L, \quad (\text{A.5})$$

$$d_{L,L} = \frac{(\alpha_H N + 1) U_L - \alpha_H N U_S}{N - \alpha_H N - 1}. \quad (\text{A.6})$$

From the assumption of $d_{S,H} > d_{S,L}$, (A.4), and (A.5), we have

$$U_L > \frac{N-1}{N} U_S. \quad (\text{A.7})$$

On the other hand, from (9), the right side of (A.6) should be equal or less than that of (A.5), and thus we have

$$U_L \leq \frac{N-1}{N} U_S. \quad (\text{A.8})$$

We confirm that (A.8) contradicts (A.7). ■

Appendix B. Derivation of conditions for C2

In this section, we divide C2 into two sub-cases: C2-a ($d_{L,L} > 0$) and C2-b ($d_{L,L} = 0$), and derive conditions for each case.

Appendix B.1. C2-a: $d_{L,L} > 0$

Focusing on the fact that the strict inequality holds in (5), we have from (19) and (20)

$$U_S < \frac{(N - \alpha_H N + \alpha_H) N}{N - 1} U_H - (1 - \alpha_H) N U_L. \quad (\text{B.1})$$

As in the derivation process in C1, we derive conditions for C2-a, which are expressed by the system parameters, from the constraints for download rate between nodes, i.e., (7)–(12). At first, from $d_{S,L} \geq 0$ in (7) and (21), we have

$$U_S \geq \alpha_H U_L. \quad (\text{B.2})$$

Noting that the right side of (20) is always positive and (19) holds, we confirm that $d_{S,H} > 0$, $d_{H,H} > 0$, and $d_{H,L} > 0$ hold in (7). From $d_{L,L} > 0$ in (7) and (22), we have

$$U_S < \frac{1}{\alpha_H} ((\alpha_H + (1 - \alpha_H)^2 N) U_L). \quad (\text{B.3})$$

In C2-a, (19) holds, and thus (8) and (10) are always satisfied. In addition, from (9), the right side of (22) should be equal or less than that of (21), which gives

$$U_S \geq \frac{N}{N-1} U_L. \quad (\text{B.4})$$

As for (11), from (19), (21), and (20), we also obtain (B.4).

So far we have all the conditions (B.1)–(B.4), which should hold at the same time. In what follows, we rearrange these conditions. At first, the difference between the right side of (B.4) and that of (B.2) gives

$$\frac{(1 - \alpha_H) N + \alpha_H}{N - 1} U_L > 0,$$

which means that (B.2) holds if (B.4) is satisfied. Next, we focus on the magnitude relationship between the right side of (B.1) and that of (B.3). If the right side of (B.1) is greater than that of (B.3), we have

$$(N - \alpha_H N + \alpha_H) \left(\frac{N}{N-1} U_H - \frac{1}{\alpha_H} U_L \right) > 0.$$

By rearranging this, we have

$$\frac{U_H}{U_L} > \frac{N-1}{\alpha_H N}. \quad (\text{B.5})$$

Otherwise, we have

$$1 < \frac{U_H}{U_L} \leq \frac{N-1}{\alpha_H N}, \quad (\text{B.6})$$

where the first inequality is given by $U_H > U_L$.

Consequently, if (B.5) holds, conditions for C2-a are (B.3) and (B.4), and otherwise they are (B.1) and (B.4).

425 *Appendix B.2. C2-b: $d_{L,L} = 0$*

Focusing on the fact that the strict inequality holds in (5), we have from (17), (23), and (24)

$$U_S < \frac{\alpha_H N(N - \alpha_H N + 1)}{\alpha_H N - 1} U_H - \frac{(1 - \alpha_H)N(\alpha_H^2 N - \alpha_H + 1)}{\alpha_H(\alpha_H N - 1)} U_L. \quad (\text{B.7})$$

As in C2-a, we derive conditions for C2-b, which are expressed by the system parameters, from the constraints for download rate between nodes, i.e., (7)–(12). At first, from $d_{S,H} \geq 0$ and $d_{H,H} \geq 0$ in (7), (17), and (24), we have

$$U_S \geq -\frac{(2\alpha_H - 1)(1 - \alpha_H)}{\alpha_H} U_L. \quad (\text{B.8})$$

From $d_{S,L} \geq 0$ in (7) and (25), we obtain

$$U_S \geq \frac{2\alpha_H - 1}{\alpha_H} U_L. \quad (\text{B.9})$$

Since the right side of (23) is positive, $d_{L,H} > 0$ in (7) always holds. In addition, $d_{L,L} \geq 0$ holds because of $d_{L,L} = 0$. So far we have all the conditions for (7).

Next, from (17), (8) holds. Because $d_{L,L} = 0$, (9) becomes the same as $d_{S,L} \geq 0$ in (7), and thus we have (B.9). Finally, we derive conditions for (10) and (11). From (10), the right side of (23) should be equal or less than that of (24), which gives

$$U_S \geq \frac{1}{\alpha_H} (\alpha_H + (1 - \alpha_H)^2 N) U_L. \quad (\text{B.10})$$

Similarly, from (11), the right side of (23) should be equal or less than that of (25), which gives

$$U_S \geq \frac{\alpha_H N + 1}{\alpha_H N} U_L. \quad (\text{B.11})$$

So far we obtain all the conditions (B.7)–(B.11), which should hold at the same time. In what follows, we rearrange these conditions. At first, the difference between the right side of (B.9) and that of (B.8) gives

$$\frac{(2\alpha_H - 1)(2 - \alpha_H)}{\alpha_H} U_L > 0,$$

which means that (B.8) holds if (B.9) is satisfied. Next, the difference between the right side of (B.11) and that of (B.9) gives

$$\frac{N - \alpha_H N + 1}{\alpha_H N} U_L > 0,$$

which indicates that (B.9) holds if (B.11) is satisfied. Similarly, the difference between the right side of (B.10) and that of (B.11) gives

$$\frac{((1 - \alpha_H)N)^2 - 1}{\alpha_H N} U_L > 0,$$

which means that (B.11) holds if (B.10) is satisfied.

As a result, both (B.10) and (B.7) should hold for C2-b, which means that the right side of (B.10) should be equal or greater than that of (B.7):

$$\frac{\alpha_H(N - \alpha_H N + 1)}{\alpha_H N - 1} \left(N U_H - \frac{N - 1}{\alpha_H} U_L \right) > 0.$$

By rearranging this, we have (B.5).

In summary, if (B.5) holds, conditions for C2-b are (B.7) and (B.10).

Appendix C. Derivation of conditions for C3

As in the other cases, we derive conditions for C3, which are expressed by the system parameters, from the constraints for download rate between nodes, i.e., (7)–(12). At first, from $d_{S,H} \geq 0$ in (7) and (26), we have

$$U_S \geq (1 - \alpha_H)N(U_H - U_L). \quad (\text{C.1})$$

Since the right side of (27) is positive, $d_{S,L} > 0$ in (7) holds.

Next, we focus on $d_{H,L} \geq 0$ in (7) and divide C3 into two sub-cases: C3-a ($d_{H,L} > 0$) and C3-b ($d_{H,L} = 0$), and derive conditions for each case.

Appendix C.1. C3-a: $d_{H,L} > 0$

We first focus on the conditions for $d_{H,L}$. From the viewpoint of high-speed peer, C3 guarantees the equality in (5), which gives $d_{H,H}$, and (26) provides $d_{S,H}$. Since $d_{H,H} \leq d_{S,H}$ should hold from (8), we have

$$d_{H,L} \geq \frac{\alpha_H(N - \alpha_H N + 1)}{(1 - \alpha_H)N} U_H - \frac{(\alpha_H N - 1)(1 - \alpha_H)}{(1 - \alpha_H)N} U_L - \frac{\alpha_H N - 1}{(1 - \alpha_H)N^2} U_S. \quad (\text{C.2})$$

Similarly, from the viewpoint of low-speed peer, C3 guarantees the equality in (6), which gives $d_{L,L}$, and (27) provides $d_{S,L}$. Since $d_{L,L} \leq d_{S,L}$ should hold from (9) and $d_{L,H} = d_{H,L}$ is satisfied in (12), we have

$$d_{H,L} \geq \frac{(\alpha_H N - 1)(1 - \alpha_H)}{\alpha_H N} U_L - \frac{\alpha_H(N - \alpha_H N - 1)}{\alpha_H N} U_H - \frac{N - \alpha_H N - 1}{\alpha_H N^2} U_S. \quad (\text{C.3})$$

(C.2) and (C.3) should hold at the same time. In what follows, we continue the analysis by considering the magnitude relationship between the right side of (C.2) and that of (C.3).

Appendix C.1.1. Constraints related to high-speed peer are dominant

In this case, the right side of (C.2) should be equal or greater than that of (C.3), and thus we have

$$\begin{aligned} & \frac{(N-1)(1-2\alpha_H)}{(1-\alpha_H)\alpha_H N^2} U_S + \frac{\alpha_H(N-\alpha_H N+2\alpha_H-1)}{(1-\alpha_H)\alpha_H N} U_H \\ & - \frac{(1-\alpha_H)(\alpha_H N-2\alpha_H+1)}{(1-\alpha_H)\alpha_H N} U_L \geq 0. \end{aligned} \quad (\text{C.4})^{450}$$

By rearranging this, if $2/N \leq \alpha_H < 1/2$, we have

$$\begin{aligned} U_S \geq & \frac{(1-\alpha_H)N(\alpha_H N-2\alpha_H+1)}{(N-1)(1-2\alpha_H)} U_L \\ & - \frac{\alpha_H N(N-\alpha_H N+2\alpha_H-1)}{(N-1)(1-2\alpha_H)} U_H, \end{aligned} \quad (\text{C.5})$$

and if $1/2 < \alpha_H \leq (N-2)/N$, we have

$$\begin{aligned} U_S < & \frac{(1-\alpha_H)N(\alpha_H N-2\alpha_H+1)}{(N-1)(1-2\alpha_H)} U_L \\ & - \frac{\alpha_H N(N-\alpha_H N+2\alpha_H-1)}{(N-1)(1-2\alpha_H)} U_H. \end{aligned} \quad (\text{C.6})$$

Note that if $\alpha_H = 1/2$, (C.4) holds. Since the right side of (C.2) should be positive from $d_{H,L} > 0$, we have

$$U_S < \frac{(N-\alpha_H N+1)\alpha_H N}{\alpha_H N-1} U_H - (1-\alpha_H)N U_L. \quad (\text{C.7})$$

So far we have confirmed that $d_{S,L} > 0$ and $d_{H,L} > 0$ in (7) and obtained the condition for $d_{S,H} \geq 0$ as (C.1). Next, we focus on the remaining conditions in (7), i.e., $d_{H,H} \geq 0$ and $d_{L,L} \geq 0$.

As for $d_{H,H}$, since $d_{H,H}$ and $d_{H,L}$ in the left side of (5) should satisfy (8) and (10) for the relationship with $d_{S,H}$, respectively, we have

$$\begin{aligned} & (\alpha_H N-1)d_{H,H} + (1-\alpha_H)N d_{H,L} \leq \\ & (\alpha_H N-1)d_{S,H} + (1-\alpha_H)N d_{S,H} = (N-1)d_{S,H}. \end{aligned}$$

In addition, considering (C.2) for $d_{H,L}$, (26) for $d_{S,H}$, and $d_{H,H} \geq 0$ in (7), we have

$$\begin{aligned} 0 \leq d_{H,H} \leq & \frac{N+\alpha_H N-2}{N(\alpha_H N-1)} U_S + \frac{N-\alpha_H^2 N+2\alpha_H-1}{\alpha_H N-1} U_H \\ & + \frac{(1-\alpha_H)(N+\alpha_H N-2)}{\alpha_H N-1} U_L. \end{aligned}$$

By rearranging this, we have

$$U_S \geq \frac{N-\alpha_H^2 N+2\alpha_H-1}{N+\alpha_H N-2} U_H - (1-\alpha_H)N U_L. \quad (\text{C.8})$$

Similarly, as for $d_{L,L}$, considering the equality in (6),⁴⁶⁰ and (C.2), we have

$$\begin{aligned} 0 \leq d_{L,L} \leq & \frac{\alpha_H(\alpha_H N-1)}{(1-\alpha_H)N(N-\alpha_H N-1)} U_S \\ & + \frac{\alpha_H(\alpha_H N-1)+1}{N-\alpha_H N-1} U_L \\ & - \frac{\alpha_H^2(N-\alpha_H N+1)}{(1-\alpha_H)(N-\alpha_H N-1)} U_H. \end{aligned} \quad (\text{C.9})$$

By rearranging this, we have

$$\begin{aligned} U_S \geq & \frac{(N-\alpha_H N+1)\alpha_H N}{\alpha_H N-1} U_H \\ & - \frac{(1-\alpha_H)N(1+\alpha_H^2 N-\alpha_H)}{\alpha_H(\alpha_H N-1)} U_L. \end{aligned} \quad (\text{C.10})$$

In addition, from (9), the right side of (C.9) should be equal or less than that of (27). By rearranging this condition, we obtain the above-mentioned conditions: i.e., (C.5) for $2/N \leq \alpha_H < 1/2$ and (C.6) for $1/2 < \alpha_H \leq (N-2)/N$.

Finally, we derive the conditions for (10) and (11). First, comparing (26) and (27), we have $d_{S,L} - d_{S,H} = U_H - U_L > 0$, and thus $d_{S,L} > d_{S,H}$ holds. As a result, (11) holds if (10) is satisfied. As for $d_{S,H}$, from (10) and (C.2), we have

$$U_S \geq \frac{(N-\alpha_H N+\alpha_H)N}{N-1} U_H - (1-\alpha_H)N U_L. \quad (\text{C.11})$$

So far we have all the conditions: (C.1), (C.7), (C.8), (C.10), and (C.11) should hold at the same time while (C.5) and (C.6) should hold for $2/N \leq \alpha_H < 1/2$ and $1/2 < \alpha_H \leq (N-2)/N$, respectively. In what follows, we rearrange these conditions. The difference between the right side of (C.11) and that of (C.1) becomes

$$\frac{N}{N-1} U_H > 0,$$

which means that (C.1) holds if (C.11) is satisfied. Similarly, the difference between the right side of (C.11) and that of (C.8) gives

$$\frac{N(\alpha_H N-1)}{(N-1)(N+\alpha_H N-2)} U_H > 0,$$

which indicates that (C.8) holds if (C.11) is satisfied.

Next, we focus on the magnitude relationship between the right side of (C.10) and that of (C.11). If the right side of (C.10) is greater than that of (C.11), we have

$$\frac{(1-\alpha_H)N^2}{(\alpha_H N-1)(N-1)} U_H - \frac{(1-\alpha_H)N}{\alpha_H(\alpha_H N-1)} U_L > 0.$$

This can be rearranged into (B.5). Otherwise, we have (B.6).

As for the remaining conditions (C.5), (C.6), and (C.7), one of (C.5) and (C.6) is satisfied depending on the value of α_H . In what follows, we derive the conditions according to the value of α_H .

Appendix C.1.1.1. $2/N \leq \alpha_H < 1/2$

In this case, (C.5) holds. If (B.5) holds, the right side of (C.10) is equal or greater than that of (C.5) when

$$\frac{\alpha_H^2 N}{(N-1)(1-2\alpha_H)} U_H - \frac{\alpha_H^2 + 1 - 2\alpha_H}{(N-1)(1-2\alpha_H)} U_L \geq 0.$$

By arranging this, we have

$$\frac{U_H}{U_L} \geq \frac{\alpha_H^2 - 2\alpha_H + 1}{\alpha_H^2 N}. \quad (\text{C.12})$$

The difference between the right side of (B.5) and that of (C.12) becomes

$$\frac{(\alpha_H N - 1) + \alpha_H(1 - \alpha_H)}{\alpha_H^2 N} > 0,$$

which indicates that (C.12) holds if (B.5) is satisfied. Consequently, (C.5) holds if (C.10) is satisfied.

On the other hand, if (B.6) holds, the difference between the right side of (C.11) and that of (C.5) becomes ⁴⁸⁰

$$\frac{(1 - \alpha_H)\alpha_H N^2}{(N - 1)(1 - 2\alpha_H)}(U_H - U_L) > 0,$$

which means that (C.5) holds if (C.11) is satisfied.

⁴⁶⁵ Consequently, the conditions for C3 in case of $2/N \leq 485$ $\alpha_H < 1/2$ are summarized as follows: If (B.5) holds, they are (C.7) and (C.10), and otherwise, they are (C.7) and (C.11).

Appendix C.1.1.2. $1/2 < \alpha_H \leq (N - 2)/N$ ⁴⁹⁰

In this case, (C.6) holds. We first confirm that the condition that the difference between the right side of (C.6) and that of (C.7) is equal or greater than zero results in

$$\frac{U_H}{U_L} \geq \frac{(1 - \alpha_H)(\alpha_H N - 1)}{(N - \alpha_H N - 1)\alpha_H}, \quad (\text{C.13})$$

which indicates that (C.6) holds if (C.7) is satisfied. Similarly, we confirm that the condition that the right side of (C.6) is less than that of (C.7) yields

$$1 < \frac{U_H}{U_L} < \frac{(1 - \alpha_H)(\alpha_H N - 1)}{(N - \alpha_H N - 1)\alpha_H}, \quad (\text{C.14})$$

⁴⁷⁰ where the first inequality comes from $U_H > U_L$. This means that (C.7) holds if (C.6) is satisfied.

So far the conditions can be summarized as follows: (((B.5) and (C.10)) or ((B.6) and (C.11))) and (((C.13) and (C.7)) or ((C.14) and (C.6))). Focusing on the four ⁴⁷⁵ conditions related to U_H/U_L , i.e., (B.5), (B.6), (C.13), and (C.14), we have to judge the magnitude relationship between the right side of (B.5) and the right side of (C.13) as well as that between the right side of (B.6) and the right side of (C.14).

The right side of (B.5) is equal or greater than that of (C.13) when

$$\frac{N((1 - \alpha_H)^2 N - 1) + 1}{((1 - \alpha_H)N - 1)\alpha_H N} \geq 0.$$

By rearranging this with the assumption of $2 \leq \alpha_H N$ and $N \geq 4$, we have

$$\frac{2}{N} \leq \alpha_H \leq 1 - \frac{\sqrt{N - 1}}{N}.$$

In addition, focusing on the fact that $2/N \leq 1/2 < 1 - \frac{\sqrt{N - 1}}{N}$ holds under $N \geq 4$, we can rearrange the condition for α_H as follows:

$$\frac{1}{2} < \alpha_H \leq 1 - \frac{\sqrt{N - 1}}{N}, \quad (\text{C.15})$$

which indicates that (C.13) holds if (B.5) is satisfied. On the other hand, if the right side of (B.5) is less than that of (C.13), using $\alpha_H N \leq N - 2$, $N \geq 4$, we have

$$1 - \frac{\sqrt{N - 1}}{N} < \alpha_H \leq 1 - \frac{2}{N}. \quad (\text{C.16})$$

Note that (C.16) holds only when $N \geq 5$. Since we are more interested in the performance of large-scale systems, we assume $N \geq 5$ in what follows. In this case, (B.5) holds if (C.13) is satisfied.

Consequently, the conditions for C3 in case of $1/2 < \alpha_H \leq (N - 2)/N$ as summarized as follows: If (C.15) holds, ((B.5) and (C.7) and (C.10))) or ((C.13) and (B.6) and (C.7) and (C.11)) or ((C.14) and (C.6) and (C.11)), and otherwise, ((C.13) and (C.7) and (C.10)) or ((C.14) and (B.5) and (C.6) and (C.10)) or ((C.14) and (C.6) and (C.11)).

Appendix C.1.1.3. $\alpha_H = 1/2$

In this case, (C.4) holds, and thus the conditions for high-speed peer are dominant. The required conditions are given by (C.1) and (C.7)–(C.11). Rearranging these conditions in a similar way in the above, we obtain the conditions for C3 in case of $\alpha_H = 1/2$ as follows: If (B.5) holds, (C.7) and (C.10), and otherwise, (C.7) and (C.11).

Appendix C.1.2. Constraints related to low-speed peer are dominant

In this case, (C.4) does not holds. In case of $2/N \leq \alpha_H < 1/2$, we have

$$U_S < \frac{(1 - \alpha_H)N(\alpha_H N - 2\alpha_H + 1)}{(N - 1)(1 - 2\alpha_H)}U_L - \frac{\alpha_H N(N - \alpha_H N + 2\alpha_H - 1)}{(N - 1)(1 - 2\alpha_H)}U_H, \quad (\text{C.17})$$

while we have

$$U_S \geq \frac{(1 - \alpha_H)N(\alpha_H N - 2\alpha_H + 1)}{(N - 1)(1 - 2\alpha_H)}U_L - \frac{\alpha_H N(N - \alpha_H N + 2\alpha_H - 1)}{(N - 1)(1 - 2\alpha_H)}U_H \quad (\text{C.18})$$

in case of $1/2 < \alpha_H \leq (N - 2)/N$. Here, from $d_{H,L} > 0$, the right side of (C.3) should be positive, and thus we have

$$U_S < \frac{(\alpha_H N + 1)(1 - \alpha_H)N}{N - \alpha_H N - 1}U_L - \alpha_H N U_H. \quad (\text{C.19})$$

As in Appendix C.1.1, we have confirmed that $d_{S,L} > 0$ and $d_{H,L} > 0$ in (7) and derived the condition for $d_{S,H} \geq 0$

as (C.1). Therefore, we will focus on the remaining constraints $d_{L,L} \geq 0$ and $d_{H,H} \geq 0$. At first, as for $d_{L,L}$, since $d_{L,L}$ and $d_{L,H}$ in the left side of (6) have the relationship (9) and (10) with $d_{S,L}$ and $d_{S,H}$, respectively, we have

$$\begin{aligned} & ((1 - \alpha_H)N - 1)d_{L,L} + \alpha_H N d_{L,H} \leq \\ & ((1 - \alpha_H)N - 1)d_{S,L} + \alpha_H N d_{S,H}. \end{aligned}$$

Here, (C.3), (26), and (27) hold for $d_{L,H}$, $d_{S,H}$, and $d_{S,L}$, respectively, and thus we have

$$\begin{aligned} 0 \leq d_{L,L} \leq & \frac{2N - \alpha_H N - 2}{N(N - \alpha_H N - 1)} U_S + \frac{\alpha_H(N - \alpha_H N - 2)}{N(N - \alpha_H N - 1)} U_H \\ & - \frac{\alpha_H(N - \alpha_H N - 2) + 1}{N(N - \alpha_H N - 1)} U_L. \end{aligned}$$

By rearranging this, we have

$$\begin{aligned} U_S \geq & - \frac{\alpha_H N(N - \alpha_H N - 2)}{2N - \alpha_H N - 2} U_H \\ & + \frac{\alpha_H N(N - \alpha_H N - 2) + N}{2N - \alpha_H N - 2} U_L. \quad (\text{C.20})^{505} \end{aligned}$$

Next, as for $d_{H,H}$, from the equality in (5), (7), and (C.3), we have

$$\begin{aligned} 0 \leq d_{H,H} \leq & \frac{(1 - \alpha_H)(N - \alpha_H N - 1)}{\alpha_H N(\alpha_H N - 1)} U_S \\ & + \frac{(1 - \alpha_H)(N - \alpha_H N - 1) + 1}{\alpha_H N - 1} U_H \\ & - \frac{(1 - \alpha_H)(1 + \alpha_H N - \alpha_H^2 N - \alpha_H)}{\alpha_H(\alpha_H N - 1)} U_L. \quad (\text{C.21}) \end{aligned}$$

By rearranging this, we have

$$\begin{aligned} U_S \geq & \frac{(\alpha_H N + 1)(1 - \alpha_H)N}{N - \alpha_H N - 1} U_L \\ & - \frac{(N - 2\alpha_H N + \alpha_H^2 N + \alpha_H)\alpha_H N}{(1 - \alpha_H)(N - \alpha_H N - 1)} U_H. \quad (\text{C.22}) \end{aligned}$$

In addition, from (8), the right side of (C.21) should be equal or less than that of (27). By rearranging this condition, we obtain the above-mentioned conditions: i.e., if $2/N \leq \alpha_H < 1/2$ holds, (C.17), and otherwise, (C.18). Finally, we derive the conditions for (10) and (11). Since $d_{S,L} > d_{S,H}$ holds, (11) holds if (10) is satisfied. As for $d_{S,H}$, from (10) and (C.3), we have

$$U_S \geq \frac{\alpha_H N}{N - 1} U_H + \frac{(1 - \alpha_H)N}{N - 1} U_L. \quad (\text{C.23})$$

So far we have all the constraints: (C.19), (C.20), (C.22), and (C.23) should hold at the same time while (C.17) and (C.18) should hold for $2/N \leq \alpha_H < 1/2$ and $1/2 < \alpha_H \leq (N - 2)/N$, respectively. In what follows, we rearrange these conditions.

At first, the difference between the right side of (C.23) and that of (C.20) becomes

$$\begin{aligned} & \frac{\alpha_H N^2(N - \alpha_H N - 1)}{(N - 1)(2N - \alpha_H N - 2)} U_H \\ & + \frac{-\alpha_H N^2(N - \alpha_H N) + N(N - 1)}{(N - 1)(2N - \alpha_H N - 2)} U_L. \end{aligned}$$

From $U_H > U_L$, this lower bound is given by

$$\frac{N(N - \alpha_H N - 1)}{(N - 1)(2N - \alpha_H N - 2)} U_L,$$

which becomes positive, and thus (C.20) holds if (C.23) is satisfied. Next, the difference between the right side of (C.23) and that of (C.22) becomes

$$\begin{aligned} & \frac{\alpha_H N^3(1 - \alpha_H)^2 + (\alpha_H N)^2}{(1 - \alpha_H)(N - 1)(N - \alpha_H N - 1)} U_H \\ & - \frac{\alpha_H N^3(1 - \alpha_H)^2}{(1 - \alpha_H)(N - 1)(N - \alpha_H N - 1)} U_L > 0, \end{aligned}$$

which indicates that (C.22) holds if (C.23) is satisfied.

The remaining conditions are (C.17), (C.18), and (C.19). Since one of (C.17) and (C.18) holds depending on the value of α_H , in what follows, we consider each case.

Appendix C.1.2.1. $2/N \leq \alpha_H < 1/2$

In this case, (C.17) holds. If the right side of (C.19) is equal or greater than that of (C.17), we have

$$\begin{aligned} & \frac{(\alpha_H N)^2}{(N - 1)(1 - 2\alpha_H)} U_H \\ & - \frac{(1 - \alpha_H)(\alpha_H N - 1)\alpha_H N^2}{(N - 1)(1 - 2\alpha_H)(N - \alpha_H N - 1)} U_L \geq 0. \end{aligned}$$

By arranging this, we obtain (C.13), and thus (C.19) holds if (C.17) is satisfied.

Therefore, from (C.13), U_S should be equal or greater than the right side of (C.23) as well as less than the right side of (C.17). However, the difference between the right side of (C.17) and that of (C.23) becomes

$$- \frac{(1 - \alpha_H)\alpha_H N^2}{(N - 1)(1 - 2\alpha_H)} (U_H - U_L), \quad (\text{C.24})$$

which is negative in case of $2/N \leq \alpha_H < 1/2$. Thus, a contradiction occurs. In other words, if (C.13) holds in case of $2/N \leq \alpha_H < 1/2$, there is no feasible parameter setting.

On the other hand, if the right side of (C.19) is less than that of (C.17), we obtain (C.14), which indicates that (C.17) holds if (C.19) is satisfied. From $U_H > U_L$, the difference between the right side of (C.14) and one should be greater than one, however, it becomes

$$- \frac{1 - 2\alpha_H}{(N - \alpha_H N - 1)\alpha_H},$$

which is negative in case of $2/N \leq \alpha_H < 1/2$. Therefore, there is no feasible parameter settings satisfying (C.14).

Appendix C.1.2.2. $1/2 < \alpha_H \leq (N-2)/N$

In this case, (C.18) holds. The difference between the right side of (C.18) and that of (C.23) becomes (C.24), which is positive in case of $1/2 < \alpha_H \leq (N-2)/N$. Therefore, the conditions for C3 in case of $1/2 < \alpha_H \leq (N-2)/N$ require that U_S should be equal or greater than the right side of (C.18) as well as less than the right side of (C.19). In this case, if the right side of (C.19) is greater than that of (C.18), we have

$$\frac{(\alpha_H N)^2}{(N-1)(1-2\alpha_H)} U_H - \frac{(1-\alpha_H)(\alpha_H N-1)\alpha_H N^2}{(N-1)(1-2\alpha_H)(N-\alpha_H N-1)} U_L > 0. \quad 530$$

By arranging this, we have (C.14).

Consequently, the conditions for C3 in case of $1/2 < \alpha_H \leq (N-2)/N$ are (C.18) and (C.19) if (C.14) is satisfied.

Appendix C.2. C3-b: $d_{H,L} = 0$

From $d_{H,L} = 0$ and the equality in (5), we have

$$d_{H,H} = \frac{U_H}{\alpha_H N - 1}. \quad (C.25)$$

Similarly, the equality in (6) gives

$$d_{L,L} = \frac{U_L}{(1-\alpha_H)N-1}. \quad (C.26)$$

Therefore, the download rate between each pair of peers is uniquely determined in this case. From $U_H > U_L > 0$ and $2 \leq \alpha_H N \leq N-2$, (C.25) and (C.26) become positive, which indicates that $d_{H,H} > 0$ and $d_{L,L} > 0$ hold in (7).

As in the other cases, we derive the conditions for C3-b based on the system parameters from the constraints related to download rate between nodes, i.e., (7)–(12). From $d_{H,L} = 0$, (10) and (11) are equivalent to (7). From (26) and (C.25), (8) can be rewritten as

$$U_S \geq \frac{(N-\alpha_H N+1)\alpha_H N}{\alpha_H N-1} U_H - (1-\alpha_H) N U_L. \quad (C.27) \quad 540$$

Note that from $d_{H,H} > 0$, $d_{S,H} > 0$ holds if (C.27) is satisfied. So far we have confirmed or obtained the conditions of (7) for all pairs of nodes. Similarly, from (27) and (C.26), (9) is rewritten as

$$U_S \geq \frac{(\alpha_H N+1)(1-\alpha_H)N}{N-\alpha_H N-1} U_L - \alpha_H N U_H. \quad (C.28) \quad 550$$

Since (C.1), (C.27), and (C.28) should hold at the same time, we focus on the magnitude relationship among the right side of these inequalities. First, the difference between the right side of (C.27) and that of (C.1) becomes

$$\frac{N}{\alpha_H N-1} U_H > 0, \quad 560$$

which indicates that (C.1) holds if (C.27) is satisfied. Therefore, we focus on the difference between the right side of (C.27) and that of (C.28). If the difference is equal or greater than zero, we have

$$\frac{\alpha_H N^2}{\alpha_H N-1} U_H - \frac{(1-\alpha_H)N^2}{N-\alpha_H N-1} U_L \geq 0.$$

By rearranging this, we have (C.13). On the other hand, if the right side of (C.27) is less than that of (C.28), noting that $U_H > U_L$, we have (C.14).

Consequently, the conditions for C3-b are summarized as follows: (C.13) and (C.27) or (C.14) and (C.28).

Appendix C.3. Integration of conditions for C3-a and C3-b

The obtained conditions for C3-a and C3-b can be summarized as Tables C.4 and C.5, respectively. From these tables, we observe that the conditions for C3-a and C3-b are independent of α_H . In addition, remember that the minimum distribution time of TFT model is identical in both C3-a and C3-b. (See Section 4.3.) Therefore, we integrate the conditions for C3-a and C3-b into those for C3 as follows. If (B.5) holds, we have

$$U_S \geq \frac{\alpha_H N(N-\alpha_H N+1)}{\alpha_H N-1} U_H - \frac{(1-\alpha_H)N(\alpha_H^2 N-\alpha_H+1)}{\alpha_H(\alpha_H N-1)} U_L,$$

and if (B.6) holds, we have

$$U_S \geq \frac{(N-\alpha_H N+\alpha_H)N}{N-1} U_H - (1-\alpha_H) N U_L.$$

References

- [1] Ubuntu, Available at <https://ubuntu.com/>.
- [2] Deploy and Update Windows 10, Available at <https://docs.microsoft.com/en-us/windows/deployment/>.
- [3] B. Zhang, A. Iosup, J. Pouwelse, D. Epema, Identifying, Analyzing, and Modeling Flashcrowds in BitTorrent, in: Proc. of IEEE P2P, 2011, pp. 240–249. doi:10.1109/P2P.2011.6038742.
- [4] F. Azzedin, M. Yahaya, Modeling BitTorrent Choking Algorithm Using Game Theory, Future Generation Computing Systems 55 (2016) 255–265. doi:10.1016/j.future.2015.02.007.
- [5] BitTorrent, Available at <https://www.bittorrent.com>.
- [6] R. L. Xia, J. K. Muppala, A Survey of BitTorrent Performance, IEEE Communications Surveys & Tutorials 12 (2) (2010) 140–158. doi:10.1109/SURV.2010.021110.00036.
- [7] M. Hasegawa, M. Sasabe, T. Takine, Analysis of Optimal Scheduling in Tit-for-Tat-Based P2P File Distribution, IEICE Transactions on Communications E97.B (12) (2014) 2650–2657. doi:10.1587/transcom.E97.B.2650.
- [8] M. Sasabe, Topological Influence on Optimality of Tit-for-Tat based P2P Content Distribution, Peer-to-Peer Networking and Applications 13 (1) (2020) 243–254. doi:10.1007/s12083-019-00763-x.
- [9] Y. Nishi, M. Sasabe, S. Kasahara, Optimality Analysis of Locality-Aware Tit-for-Tat-Based P2P File Distribution, Peer-to-Peer Networking and Applications 13 (5) (2020) 1688–1703. doi:10.1007/s12083-020-00925-2.

Table C.4: Conditions for C3-a where $d_{H,L} > 0$ ($\theta_1 = \frac{N-1}{\alpha_H N}$, $\theta_2 = \frac{(1-\alpha_H)(\alpha_H N-1)}{\alpha_H(N-\alpha_H N-1)}$, $N \geq 5$).

Case: $\frac{2}{N} < \alpha_H \leq \frac{1}{2}$	
Case: $\theta_1 < \frac{U_H}{U_L}$	$\frac{(N-\alpha_H N+1)\alpha_H N}{\alpha_H N-1} U_H - \frac{(1-\alpha_H)N(\alpha_H^2 N-\alpha_H+1)}{\alpha_H(\alpha_H N-1)} U_L \leq U_S < \frac{(N-\alpha_H N+1)\alpha_H N}{\alpha_H N-1} U_H - (1-\alpha_H)N U_L$
Case: $\theta_2 \leq \frac{U_H}{U_L} \leq \theta_1$	$\frac{(N-\alpha_H N+\alpha_H)N}{N-1} U_H - (1-\alpha_H)N U_L \leq U_S < \frac{(N-\alpha_H N+1)\alpha_H N}{\alpha_H N-1} U_H - (1-\alpha_H)N U_L$
Case: $\frac{1}{2} < \alpha_H \leq 1 - \frac{\sqrt{N-1}}{N}$	
Case: $\theta_1 < \frac{U_H}{U_L}$	$\frac{(N-\alpha_H N+1)\alpha_H N}{\alpha_H N-1} U_H - \frac{(1-\alpha_H)N(\alpha_H^2 N-\alpha_H+1)}{\alpha_H(\alpha_H N-1)} U_L \leq U_S < \frac{(N-\alpha_H N+1)\alpha_H N}{\alpha_H N-1} U_H - (1-\alpha_H)N U_L$
Case: $\theta_2 \leq \frac{U_H}{U_L} \leq \theta_1$	$\frac{(N-\alpha_H N+\alpha_H)N}{N-1} U_H - (1-\alpha_H)N U_L \leq U_S < \frac{(N-\alpha_H N+1)\alpha_H N}{\alpha_H N-1} U_H - (1-\alpha_H)N U_L$
Case: $1 < \frac{U_H}{U_L} < \theta_2$	$\frac{(N-\alpha_H N+\alpha_H)N}{N-1} U_H - (1-\alpha_H)N U_L \leq U_S < \frac{(\alpha_H N+1)(1-\alpha_H)N}{N-\alpha_H N-1} U_L - \alpha_H N U_H$
Case: $1 - \frac{\sqrt{N-1}}{N} < \alpha_H \leq 1 - \frac{2}{N}$	
Case: $\theta_2 \leq \frac{U_H}{U_L}$	$\frac{(N-\alpha_H N+1)\alpha_H N}{\alpha_H N-1} U_H - \frac{(1-\alpha_H)N(\alpha_H^2 N-\alpha_H+1)}{\alpha_H(\alpha_H N-1)} U_L \leq U_S < \frac{(N-\alpha_H N+1)\alpha_H N}{\alpha_H N-1} U_H - (1-\alpha_H)N U_L$
Case: $\theta_1 < \frac{U_H}{U_L} < \theta_2$	$\frac{(N-\alpha_H N+1)\alpha_H N}{\alpha_H N-1} U_H - \frac{(1-\alpha_H)N(\alpha_H^2 N-\alpha_H+1)}{\alpha_H(\alpha_H N-1)} U_L \leq U_S < \frac{(\alpha_H N+1)(1-\alpha_H)N}{N-\alpha_H N-1} U_L - \alpha_H N U_H$
Case: $1 < \frac{U_H}{U_L} \leq \theta_1$	$\frac{(N-\alpha_H N+\alpha_H)N}{N-1} U_H - (1-\alpha_H)N U_L \leq U_S < \frac{(\alpha_H N+1)(1-\alpha_H)N}{N-\alpha_H N-1} U_L - \alpha_H N U_H$

Table C.5: Conditions for C3-b where $d_{H,L} = 0$ ($\theta_2 = \frac{(1-\alpha_H)(\alpha_H N-1)}{\alpha_H(N-\alpha_H N-1)}$).

Case: $\theta_2 \leq \frac{U_H}{U_L}$	$U_S \geq \frac{(N-\alpha_H N+1)\alpha_H N}{\alpha_H N-1} U_H - (1-\alpha_H)N U_L$
Case: $1 < \frac{U_H}{U_L} < \theta_2$	$U_S \geq \frac{(\alpha_H N+1)(1-\alpha_H)N}{N-\alpha_H N-1} U_L - \alpha_H N U_H$

- [10] M. Sasabe, Analysis of Minimum Distribution Time of Tit-for-Tat-Based P2P File Distribution: Linear Programming Based Approach, Peer-to-Peer Networking and Applications (2021) 1–605 21 (to appear).
- [11] IBM ILOG CPLEX Optimizer, Available at <https://www.ibm.com/analytics/cplex-optimizer>.
- [12] R. Kumar, K. W. Ross, Peer-Assisted File Distribution: The Minimum Distribution Time, in: Proc. of 1st IEEE Workshop⁶¹⁰ on Hot Topics in Web Systems and Technologies, 2006, pp. 1–11. doi:10.1109/HOTWEB.2006.355259.
- [13] D. Stutzbach, R. Rejaie, Understanding Churn in Peer-to-Peer Networks, in: Proc. of the 6th ACM SIGCOMM Conference on Internet Measurement, 2006, pp. 189–202. doi:10.1145/⁶¹⁵1177080.1177105.
- [14] F. L. Haddi, M. Benchaïba, A Survey of Incentive Mechanisms in Static and Mobile P2P Systems, Journal of Network and Computer Applications 58 (2015) 108–118. doi:10.1016/j.jnca.2015.09.004.
- [15] M. D. Samuel, R. Balakrishnan, A Grade-based Incentive Mechanism with Starvation Prevention for Maintaining Fairness in Peer-to-Peer Networks, International Journal of System Assurance Engineering and Management 3 (2) (2012) 84–99. doi:10.1007/s13198-012-0098-5.
- [16] M. J. Neely, L. Golubchik, Utility Optimization for Dynamic Peer-to-Peer Networks with Tit-for-Tat Constraints, in: Proc. of IEEE INFOCOM, 2011, pp. 1458–1466. doi:10.1109/INFCOM.2011.5934933.
- [17] R. Zhou, K. Hwang, M. Cai, GossipTrust for Fast Reputation⁶³⁰ Aggregation in Peer-to-Peer Networks, IEEE Transactions on Knowledge and Data Engineering 20 (9) (2008) 1282–1295. doi:10.1109/TKDE.2008.48.
- [18] F. N. Nwebonyi, R. Martins, M. E. Correia, Reputation based Approach for Improved Fairness and Robustness in P2P Pro-⁶³⁵ tocols, Peer-to-Peer Networking and Applications 12 (4) (2019) 951–968. doi:10.1007/s12083-018-0701-x.
- [19] N. Anjum, D. Karamshuk, M. Shikh-Bahaei, N. Sastry, Survey on Peer-Assisted Content Delivery Networks, Computer Networks 116 (2017) 79–95. doi:10.1016/j.comnet.2017.02.008.
- [20] B. Zolfaghari, G. Srivastava, S. Roy, H. R. Nemati, F. Afghah, T. Koshiha, A. Razi, K. Bibak, P. Mitra, B. K. Rai, Content Delivery Networks: State of the Art, Trends, and Future Roadmap, ACM Computing Surveys 53 (2) (2020) 34:1–34:34. doi:10.1145/3380613.
- [21] D. Qiu, R. Srikant, Modeling and Performance Analysis of BitTorrent-like Peer-to-Peer Networks, ACM SIGCOMM Computer Communication Review 34 (4) (2004) 367–378. doi:10.1145/1030194.1015508.
- [22] F. Murai, A. A. d. A. Rocha, D. R. Figueiredo, E. A. de Souza e Silva, Heterogeneous Download Times in a Homogeneous BitTorrent Swarm, Computer Networks 56 (7) (2012) 1983–2000. doi:10.1016/j.comnet.2012.02.009.
- [23] E. de Souza e Silva, R. M. M. Leão, D. S. Menasché, D. Towsley, On the Scalability of P2P Swarming Systems, Computer Networks 151 (2019) 93–113. doi:10.1016/j.comnet.2019.01.006.
- [24] C. Carbutaru, Y. M. Teo, B. Leong, T. Ho, Modeling Flash Crowd Performance in Peer-to-Peer File Distribution, IEEE Transactions on Parallel and Distributed Systems 25 (10) (2014) 2617–2626. doi:10.1109/TPDS.2013.220.
- [25] C. Carbutaru, Y. M. Teo, Analysis of Server Distribution Policies in Peer-Assisted File Distribution with Flash Crowds, in: S. Tanaka, K. Hasegawa, R. Xu, N. Sakamoto, S. J. Turner (Eds.), AsiaSim 2014, Vol. 474, Springer Berlin Heidelberg, Berlin, Heidelberg, 2014, pp. 48–61. doi:10.1007/978-3-662-45289-9_5.
- [26] A. Ferragut, F. Paganini, Fluid Models of Population and Download Progress in P2P Networks, IEEE Transactions on Control of Network Systems 3 (1) (2016) 34–45. doi:10.1109/TCNS.2015.2434092.
- [27] X. Meng, P.-S. Tsang, K.-S. Lui, Analysis of Distribution Time of Multiple Files in a P2P Network, Computer Networks 57 (15) (2013) 2900–2915. doi:10.1016/j.comnet.2013.06.015.
- [28] PlanetLab, Available at <https://planetlab.cs.princeton.edu/>.
- [29] L. Peterson, T. Roscoe, The Design Principles of PlanetLab, ACM SIGOPS Operating Systems Review 40 (1) (2006) 11–16. doi:10.1145/1113361.1113367.
- [30] D. DeFigueiredo, B. Venkatchalam, S. F. Wu, Bounds on the Performance of P2P Networks Using Tit-for-Tat Strategies, in: Proc. of IEEE P2P, 2007, pp. 11–18. doi:10.1109/P2P.2007.32.
- [31] M. Sasabe, Analysis of Optimal Piece Flow in Tit-for-Tat-Based P2P Streaming, Computer Networks 139 (2018) 60–69. doi:10.1016/j.comnet.2018.04.004.